Initiation of the West Antarctic Ice Sheet and estimates of total Antarctic ice volume in the earliest Oligocene

Douglas S. Wilson,[1] David Pollard,[2] Robert M. DeConto,[3] Stewart S.R. Jamieson,[4] and Bruce P. Luyendyk[5]

[1]   Reconstructions of Antarctic paleotopography for the late Eocene suggest that glacial erosion and thermal subsidence have lowered West Antarctic elevations considerably since then, with Antarctic land area having decreased ~20%. A new climate-ice sheet model based on these reconstructions shows that the West Antarctic Ice Sheet first formed at the Eocene-Oligocene transition (33.8–33.5 Ma, E-O) in concert with the continental-scale expansion of the East Antarctica Ice Sheet and that the total volume of East and West Antarctic ice (33.4–35.9×10^6 km^3) was >1.4 times greater than previously assumed. This larger modeled ice volume is consistent with a modest cooling of 1–2°C in the deep ocean during the E-O transition, lower than other estimates of ~3°C cooling, and suggests the possibility of substantial ice in the Antarctic interior before the Eocene-Oligocene boundary.
Citation: Wilson, D. S., D. Pollard, R. M. DeConto, S. S. R. Jamieson, and B. P. Luyendyk (2013), Initiation of the West Antarctic Ice Sheet and estimates of total Antarctic ice volume in the earliest Oligocene, *Geophys. Res. Lett.*, *40*, 4305–4309, doi:10.1002/grl.50797.

1.   Introduction

[2]   The Eocene-Oligocene (E-O) global climate transition from a warm (greenhouse) Earth to a cooler (icehouse) climate has long been recognized as being associated with growth of a significant ice sheet on Antarctica that extended to sea level [*Shackleton and Kennett*, 1975]. One main line of evidence for this is a positive shift in deep-ocean benthic foraminifera δ^{18}O of +1.0–1.5‰ [*Miller et al.*, 1987; *Shackleton and Kennett*, 1975]. As marine records have been studied with increasing resolution, the transition has been recognized to span only 300–400 kyr [*Coxall et al.*, 2005; *Katz et al.*, 2008; *Pusz et al.*, 2011; *Zachos et al.*, 1996].

[3]   A positive δ^{18}O shift can be explained by both a decrease in ocean temperature and an increase in ice volume. Therefore, substantial effort has been devoted to interpreting separate proxy records of temperature [e.g., *Liu et al.*, 2009] and sea level (ice volume) in order to determine their relative importance [e.g., *Miller et al.*, 2008a; *Miller et al.*, 2008b]. The general consensus is that the ice volume increase at the E-O is comparable to or larger than the volume of present Antarctic ice (25.4×10^6 km^3, BEDMAP [*Lythe et al.*, 2001]). Previous numerical model simulations of E-O ice growth assuming West Antarctica was mostly submarine as it is today fell significantly short of this volume (~20×10^6 km^3 [*DeConto and Pollard*, 2003b]), leading to the following question: Where was the missing ice? Subsequent studies seemed to rule out the Northern Hemisphere [*DeConto et al.*, 2008], suggesting that the modeling assumptions for Antarctica might be incorrect or that the ocean cooled more than indicated in proxy temperature studies [e.g., *Liu et al.*, 2009].

[4]   The primary factor limiting ice volume in previous E-O glaciation models was the use of modern Antarctic bedrock topography (adjusted for the removal of ice) as a boundary condition. The use of the present topography ignores the significant long-term processes of landscape evolution including glacial erosion, thermal subsidence, and tectonics, which are likely to have significantly lowered the topography. Recognizing this, recent process-based reconstructions of E-O topography [*Wilson and Luyendyk*, 2009; *Wilson et al.*, 2012] suggest that after accounting for glacial erosion and thermal subsidence, much of West Antarctica lay above sea level (Figure 1) and was therefore capable of supporting terrestrially grounded ice, even when ocean temperatures were likely too warm to support buttressing ice shelves and a marine-based West Antarctic Ice Sheet. Acknowledging large uncertainties in restoring eroded material to its original position, *Wilson et al.* [2012] offer maximum and minimum bedrock elevation reconstructions, with differences dominated by limited knowledge of the volume of post-Eocene sediment deposited around the Antarctic continental margin. Here we report on the implications of these topographic models for growth of Antarctic ice in the earliest Oligocene.

2.   Methods

[5]   We use forward modeling to predict the earliest Oligocene equilibrium ice sheet configuration for both the minimum and maximum *Wilson et al.* [2012] reconstructions and, for contrast, the modern ice-free rebounded ALBMAP v1 topography [*Le Brocq et al.*, 2010] used in previous models. The *Wilson et al.* [2012] reconstruction starts with the BEDMAP [*Lythe et al.*, 2001] topography modified for new data available in West Antarctica; for our purposes, differences between BEDMAP, ALBMAP, and the most recent BEDMAP2 [*Fretwell et al.*, 2013] topography are very minor.

[1]Department of Earth Science and Marine Science Institute, University of California, Santa Barbara, California, USA.
[2]Earth and Environmental Systems Institute, Pennsylvania State University, University Park, Pennsylvania, USA.
[3]Department of Geosciences, University of Massachusetts Amherst, Amherst, Massachusetts, USA.
[4]Department of Geography, University of Durham, Durham, UK.
[5]Department of Earth Science and Earth Research Institute, University of California, Santa Barbara, California, USA.

Corresponding author: D. S. Wilson, Department of Earth Science, University of California, 1006 Webb Hall, Santa Barbara, CA 93106-9630, USA. (dwilson@geol.ucsb.edu)
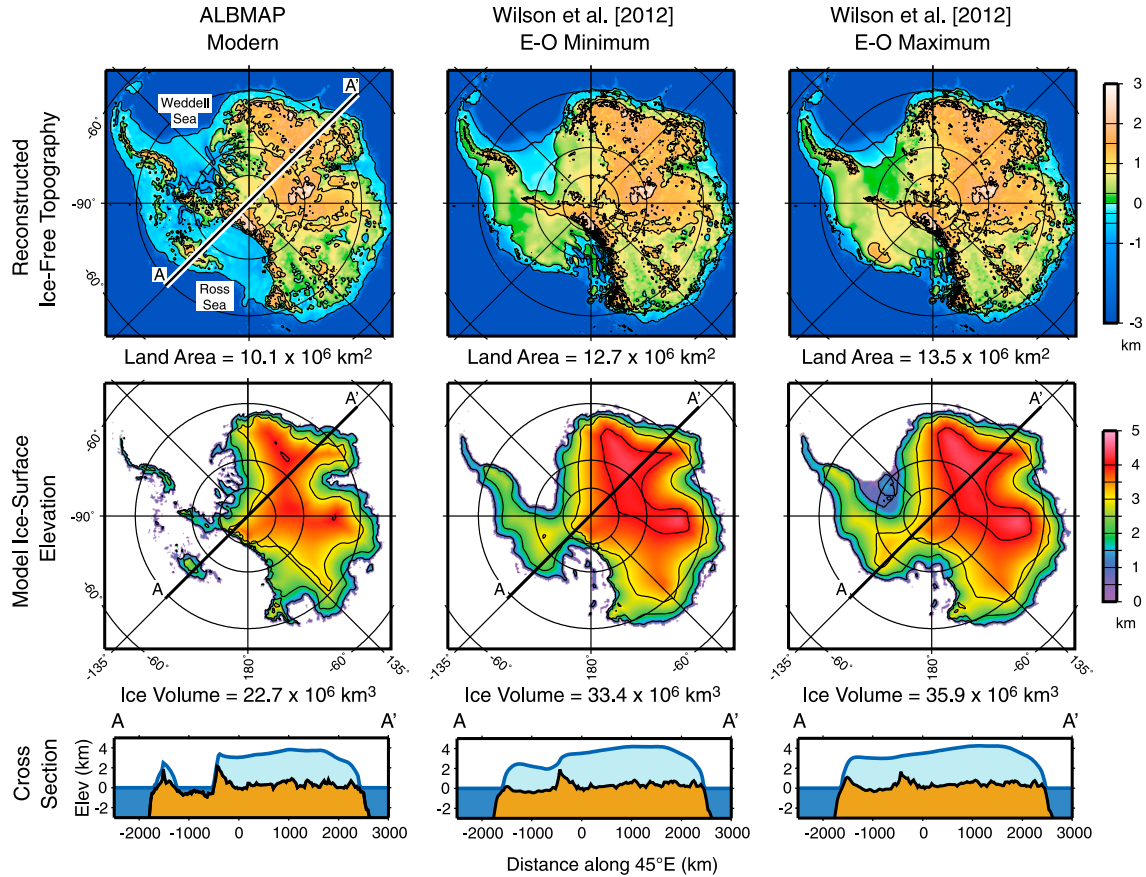
Figure 1. (top) Reconstructed ice-free topography from ALBMAP modern topography [*Le Brocq et al.*, 2010] and minimum and maximum estimates for E-O topography from *Wilson et al.* [2012], along with corresponding modeled E-O ice sheets in (middle) map view and (bottom) cross section. Greater area of land above sea level in the reconstructed topography accommodates significantly greater ice volume than modern ice-free rebounded topography because in the latter, much of West Antarctica is submerged and the (assumed) warm E-O ocean does not allow the growth of any marine ice.

[6] For each of the topographic reconstructions, we simulate ice growth using a 3-D ice sheet-shelf model on a 20 km grid [*Pollard and DeConto*, 2009; *Pollard and DeConto*, 2012]. Model parameters include surface mass balance derived from GENESIS v3 global climate model (GCM) climate simulations, a slab mixed-layer ocean, E-O global paleogeography, CO_2 at $2.5 \times PAL$ (preindustrial atmospheric level), and constant, average orbital parameters [*Alder et al.*, 2011; *DeConto and Pollard*, 2003a; *Thompson and Pollard*, 1997]. Subice basal conditions are largely unknown in the Paleogene, so the friction coefficient for basal sliding is set everywhere for hard bedrock conditions, with one exception explained below. Assuming warm Southern Ocean temperatures, floating ice is assumed to melt instantly, which precludes the buttressing effect of ice shelves. For modern simulations, ice-free rebounded bed topography is obtained from the ALBMAP v1 data set [*Le Brocq et al.*, 2010]. The climate and ice sheet models are coupled asynchronously, in a more direct way than in *DeConto and Pollard* [2003a]. Starting from no ice and an initial GCM simulation, the ice sheet model is run for 40 kyr; then, a 30 year GCM climate run with the current ice extent determines new temperature and precipitation boundary conditions for the next 40 kyr ice sheet iteration. The models are very close to equilibrium, and the ice sheet is essentially fully grown after three or four iterations, i.e.,

after 120 to 160 kyr of ice model integration. These simulations are only intended to predict the steady state ice volume averaged over orbital cycles, not the details of the growth.

[7] Predicting the isotopic change ($\Delta \delta^{18}O$) of the ocean for a given volume of ice requires knowledge of the isotopic composition of the ice. In this study, we calculate the internal distribution of $\delta^{18}O$ in the equilibrated ice sheet. Lagrangian flow trajectories are traced backward in small increments from each internal grid cell to the ice surface, repeatedly interpolating the 3-D velocities to the current trajectory point. The $\delta^{18}O$ of precipitation at the surface location is then assigned to the grid cell, under the assumption that $\delta^{18}O$ is a conservative tracer. This method is related to the semi-Lagrangian advection of depositional provenance labels in *Clarke et al.* [2005] but is simpler because it assumes that the ice sheet is fully equilibrated with a constant climate. Both methods avoid the spurious diffusion that would result by advecting the internal $\delta^{18}O$ distribution forward as a tracer.

[8] Precipitation in the highest central region of the ice sheet is isotopically lightest, and ice accumulating in the central region spends the most time in the ice sheet. This correlation between composition and residence time yields a bulk composition for the ice about 10–11‰ lighter than the average precipitation. As in *DeConto et al.* [2008], $\delta^{18}O$ of precipitation falling on the ice sheet surface is provided by the isotopic capability in the GENESIS GCM [*Mathieu*

Table 1. Results Summary[a]

	(A) Rebounded ALBMAP Topography, E-O climate	(B) E-O Minimum Topography [*Wilson et al.*, 2012], E-O climate	(C) E-O Maximum Topography [*Wilson et al.*, 2012], E-O climate	(D) Rebounded ALBMAP Topography, Modern Climate
Ice volume (10^6 km^3)	22.7	33.4	35.9	28.0
Apparent sea level drop (m)	56.8	83.4	89.5	66.0
Modeled mean ice δ^{18}O (‰)	−42.1	−44.6	−45.4	−43.2
Change in ocean δ^{18}O (‰), case 1, no Eocene ice	0.67	1.05	1.14	n.a.
Benthic cooling (°C), case 1	2.5	1.0	0.6	n.a.
Change in ocean δ^{18}O (‰), case 2, 7×10^6 km^3 Eocene ice	0.46	0.82	0.97	n.a.
Benthic cooling (°C), case 2	3.4	1.9	1.3	n.a.

[a]Models A, B, and C are plotted in Figure 1. Model D is a validation test (allowing floating ice shelves), predicting 28.0×10^6 km^3 ice volume, compared with 26.2×10^6 km^3 observed. Volumes account for projection distortion. Two cases of predicted deep-ocean cooling follow from contrasting assumptions with and without significant ice already present in the late Eocene, both assuming observed foraminiferal $\Delta\delta^{18}$O = +1.3‰. n.a. = not applicable.

et al., 2002]. Compared to modern observed δ^{18}O in precipitation over Antarctica, the GCM values are biased positively (too heavy) by about 10‰ [*Mathieu et al.*, 2002]. Here we assume that the same bias applies for the E-O model and subtract 10‰ from all GCM Antarctic values.

3. Results

[9] Our model results confirm that the volume of the nascent Antarctic ice sheet was a direct function of land area above sea level. Predicted ice volumes are 22.7×10^6 km^3 for rebounded ALBMAP, 33.4×10^6 km^3 for the reconstructed minimum E-O topography, and 35.9×10^6 km^3 for the reconstructed maximum E-O topography (Figure 1 and Table 1, columns A–C). Corresponding apparent sea level drops (terminology of *Pekar et al.* [2002]), accounting for displacement effect of below sea level ice but neglecting isostatic adjustment and simply assuming 3.65×10^8 km^2 ocean area, are 56.8, 83.4, and 89.5 m, respectively. The maximum topography model has basal sliding coefficients increased in the low-elevation Weddell Sea drainage, appropriate for minimally consolidated sediments. A control run with rebounded ALBMAP topography and modern climate GCM, allowing floating ice shelves, predicts present-day ice volume of about 7% greater than observed (Table 1, column D). A similar slightly high bias may be present in our E-O results.

4. Discussion and Conclusions

[10] Our modeling results indicate that a predecessor of the modern West Antarctic Ice Sheet developed at the E-O transition as a result of that subcontinent being largely above sea level at that time. Most prior interpretations based on data on and around the Antarctic Peninsula have found that it initiated in either the middle Miocene [*Barker and Camerlenghi*, 2002] or at the E-O transition [*Birkenmajer et al.*, 2005; *Ivany et al.*, 2006]. We believe our model results resolve this issue in favor of the E-O interpretation. Most previous ice sheet models of Cenozoic Antarctica ice treated the landscape as a passive element of the glacial system and used present bed topography, isostatically adjusted for the removal of modern ice [e.g., *Cristini et al.*, 2012; *DeConto and Pollard*, 2003b; *Huybrechts*, 1993; *Jamieson et al.*, 2010]. However, the larger E-O ice sheets simulated here are the direct result of accounting for the significant

topographic change experienced across the continent, particularly in West Antarctica.

[11] Several recent studies have tried to reconcile conflicting proxy records for environmental changes across the E-O transition, with the main uncertainty resulting from the dependence of the δ^{18}O record on both water temperature and ice volume. For a continental shelf site in Alabama, *Katz et al.* [2008] interpreted data including benthic δ^{18}O, Mg/Ca, and foraminiferal abundances as a proxy for local water depth to indicate a global apparent sea level drop of ~105 m (equivalent to growth of ~45×10^6 km^3 of ice), assuming ice composition at −45‰. *Liu et al.* [2009] focused on direct temperature proxies and found a drop of 5°C for surface waters at high northern latitudes. Their modeling studies indicated that this surface cooling would correspond to 3–5°C of deepwater cooling. *Pusz et al.* [2011] studied deepwater records from the South Atlantic (Ocean Drilling Program Sites 1090 and 1265), making an effort to correct the Mg/Ca temperature proxy for biases resulting from changes in carbonate ion concentration. They determined a two-step cooling history with a 2°C cooling early in the transition (~33.9 Ma) and a less certain cooling of ~1.5°C late in the transition (~33.5 Ma). Assuming ice δ^{18}O composition of −45 to −50‰, they inferred that the earliest Oligocene ice sheet was close to the modern volume.

[12] To compare our results to previous proxy estimates, we compute benthic cooling from the ocean $\Delta\delta^{18}$O predicted from ice volume and composition, and a cooling coefficient of 4°/‰ (Table 1). The resulting predictions are less than the 3°C minimum cooling interpreted by *Liu et al.* [2009] and *Pusz et al.* [2011], even allowing for a possible bias that our models overpredict ice volume by up to 10%. The disagreement is smallest for an isotopically heavy ice sheet and the minimum reconstructed topography. One source of uncertainty in ice volume reconstructions is the assumed hard bedrock basal conditions. It is possible that a deep, deformable regolith layer covered most of the continent in the Eocene and took several million years to erode after the ice sheet formed [*DeConto and Pollard*, 2003b]. A more deformable bed would lead to predictions of lower ice volume and more benthic cooling for a given δ^{18}O shift.

[13] Another possibility is that there were significant ice sheets covering high elevations for much of the late Eocene, so the change in ice volume and resultant δ^{18}O shift over the E-O transition would be smaller. The simulation of *DeConto and Pollard* [2003b], assuming steadily declining

CO_2 through the E-O transition, shows East Antarctica covered with ice at elevations above about 1400 m ($CO_2 = 2.96 \times$ PAL; their Figure 3b) before the continent became fully glaciated at $CO_2 = 2.8 \times$ PAL (their Figure 3d). These precursory, high-elevation ice caps fluctuated between about 5 and 9×10^6 km^3 (their Figure 2a) in response to orbital forcing. The corresponding $\delta^{18}O$ variability of 0.1‰ would be at about the noise level in the benthic isotope record. The rebounded land area above 1400 m covers 2.0×10^6 km^2 in BEDMAP and 2.1 to 2.3×10^6 km^2 in the reconstructed models, so over 80% of the continent remains below 1400 m. This enabled a two-phase ice volume expansion, with initial substantial ice accumulating on high-elevation terrain before long-term cooling triggered the albedo and height-mass balance feedbacks that led to extremely rapid continental ice growth at the end of the E-O transition.

[14] Recalculating deep sea temperatures assuming a preexisting 7×10^6 km^3 Eocene ice sheet results in 1–2°C of cooling (Table 1, case 2) at the E-O transition, which is closer to observations. At the same time, substantial ice volume prior to the main transition reduces the potential eustatic sea level fall during the transition, making the fit with available sea level estimates worse. Although there has been only passing mention of stable Antarctic ice sheets in the late Eocene [e.g., *Zachos et al.*, 1996; *Zachos et al.*, 2001], we suggest that potential high-elevation ice sheets of significant volume need to be considered in reconciling the various proxy records for the E-O transition, which should include glaciohydroisostatic adjusted sea level estimates [*Stocchi et al.*, 2013]. The presence of localized ephemeral or stable late Eocene ice sheets with cold-based, nonerosive cores and warm-based valley glaciers extending from mountain ridges is consistent with analysis of the topography of the Gamburtsev Subglacial Mountains [*Rose et al.*, 2013].

[15] Fully resolving the conflicting proxy contributions is beyond the scope of this paper, especially considering the limited understanding of the uncertainties in each proxy. Our results show that greater reconstructed Antarctic land area for the late Eocene implies that "missing ice" is no longer a problem. Future work will focus on resolving whether our E-O transition ice volumes are too large, whether the initial ice sheet was isotopically heavier than we assume, or whether the volume of high-elevation late Eocene ice caps was larger than the current evidence suggests. An earliest Oligocene Antarctic ice volume larger than the modern ice sheet is consistent with a large sea level drop and modest benthic cooling.

References

Alder, J. R., S. W. Hostetler, D. Pollard, and A. Schmittner (2011), Evaluation of a present-day climate simulation with a new coupled atmosphere-ocean model GENMOM, *Geosci. Model Devel.*, *3*(4), 69–83, doi:10.5194/gmd-4-69-2011.

Barker, P. F., and A. Camerlenghi (2002), Glacial history of the Antarctic Peninsula from Pacific margin sediments, *Proc. Ocean Drill. Program, Sci. Results*, *113*, 1–40.

Birkenmajer, K., A. Gaździcki, K. P. Krajewski, A. Przybycin, A. Solecki, A. Tatur, and H. I. Yoon (2005), First Cenozoic glaciers in West Antarctica, *Polish Polar Res.*, *26*(1), 3–12.

Clarke, K. C., N. Lhomme, and S. J. Marshall (2005), Tracer transport in the Greenland ice sheet: Three-dimensional isotopic stratigraphy, *Quat. Sci. Rev.*, *24*, 155–171, doi:10.1016/j.quascirev.2004.08.021.

Coxall, H. K., P. A. Wilson, H. Pälike, C. H. Lear, and J. Backman (2005), Rapid stepwise onset of Antarctic glaciation and deeper calcite compensation in the Pacific Ocean, *Nature*, *433*, 53–57, doi:10.1038/nature03135.

Cristini, L., K. Grosfeld, M. Butzin, and G. Lohmann (2012), Influence of the opening of the Drake Passage on the Cenozoic Antarctic Ice Sheet: A modeling approach, *Palaeogeogr. Palaeoclimatol. Palaeoecol*, *339-341*, 66–73, doi:10.1016/j.palaeo.2012.04.023.

DeConto, R. M., and D. Pollard (2003a), A coupled climate-ice sheet modeling approach to the Early Cenozoic history of the Antarctic ice sheet, *Palaeogeogr. Palaeoclimatol. Palaeoecol.*, *198*, 39–52, doi:10.1016/S0031-0182(03)00393-6.

DeConto, R. M., and D. Pollard (2003b), Rapid Cenozoic glaciation of Antarctica induced by declining atmospheric CO_2, *Nature*, *421*, 245–249, doi:10.1038/nature01290.

DeConto, R. M., D. Pollard, P. A. Wilson, H. Pälike, C. Lear, and M. Pagani (2008), Thresholds for Cenozoic bipolar glaciation, *Nature*, *455*, 652–657, doi:10.1038/nature07337.

Fretwell, P., et al. (2013), Bedmap2: Improved ice bed, surface and thickness datasets for Antarctica, *The Cryosphere*, *7*, 375–393, doi:10.5194/tc-7-375-2013.

Huybrechts, P. (1993), Glacial modeling of the late Cenozoic East Antarctic ice sheet: Stability or dynamism, *Geografiska Annaler, Series A*, *75A*, 221–238.

Ivany, L. C., S. Van Simaeys, E. W. Domack, and S. D. Samson (2006), Evidence for an earliest Oligocene ice sheet on the Antarctic Peninsula, *Geology*, *34*(5), 377–380, doi:10.1130/G22383.1.

Jamieson, S. S. R., D. E. Sugden, and N. R. J. Hulton (2010), The evolution of the subglacial landscape of Antarctica, *Earth Planet. Sci. Lett.*, *293*, 1–27, doi:10.1016/j.epsl.2010.02.012.

Katz, M. E., K. G. Miller, J. D. Wright, B. S. Wade, J. V. Browning, B. S. Cramer, and Y. Rosenthal (2008), Stepwise transition from the Eocene greenhouse to the Oligocene icehouse, *Nat. Geosci.*, *1*, 329–334, doi:10.1038/ngeo179.

Le Brocq, A. M., A. J. Payne, and A. Vieli (2010), An improved Antarctic dataset for high resolution numerical ice sheet models (ALBMAP v1), *Earth Syst. Sci. Data*, *2*, 247–260, doi:10.5194/essdd-3-195-2010.

Liu, Z., M. Pagani, D. Zinniker, R. DeConto, M. Huber, H. Brinkuis, S. R. Shah, R. M. Leckie, and A. Pearson (2009), Global cooling during the Eocene-Oligocene climate transition, *Science*, *323*, 1187–1190, doi:10.1126/science.1166368.

Lythe, M. B., et al. (2001), BEDMAP: A new ice thickness and subglacial topographic model of Antarctica, *J. Geophys. Res.*, *106*(6), 11,335–311,351, doi:10.1029/2000JB900449.

Mathieu, R., D. Pollard, J. E. Cole, J. W. C. White, R. S. Webb, and S. L. Thompson (2002), Simulation of stable water isotope variations by the GENESIS GCM for modern conditions, *J. Geophys. Res.*, *107*(D4), 4037, doi:10.1029/2001JD900255.

Miller, K. G., R. Fairbanks, and G. S. Mountain (1987), Tertiary oxygen isotope synthesis, sea level history and continental margin erosion, *Paleoceanography*, *2*, 1–19, doi:10.1029/PA002i001p00001.

Miller, K. G., J. D. Wright, M. E. Katz, J. V. Browning, B. S. Cramer, B. S. Wade, and S. F. Mizintseva (2008a), A view of Antarctic Ice-Sheet evolution from sea-level and deep-sea isotope changes during the Late Cretaceous-Cenozoic, in *Antarctica: A Keystone in a Changing World. Proceedings of the 10th International Symposium on Antarctic Earth Sciences*, edited by A. K. Cooper et al., pp. 55–70, The National Academies Press, Washington, DC, doi:10.3133/of2007-1047.kp3106.

Miller, K. G., J. V. Browning, M.-P. Aubry, B. S. Wade, M. E. Katz, A. A. Kulpecz, and J. D. Wright (2008b), Eocene–Oligocene global climate and sea-level changes: St. Stephens Quarry, Alabama, *Geol. Soc. Am. Bull.*, *120*(1/2), 34–53, doi:10.1130/B26105.26101.

Pekar, S. F., N. Christie-Blick, M. A. Kominz, and K. G. Miller (2002), Calibration between glacial eustasy and oxygen isotopic data for the early icehouse world of the Oligocene, *Geology*, *30*, 903–906, doi:10.1130/0091-7613(2002)030<0903:CBEEFB>2.0.CO;2.

Pollard, D., and R. M. DeConto (2009), Modelling West Antarctic ice sheet growth and collapse through the past five million years, *Nature*, *458*(7236), 329–332, doi:10.1038/nature07809.

Pollard, D., and R. M. DeConto (2012), Description of a hybrid ice sheet-shelf model, and application to Antarctica, *Geosci. Model Devel.*, *5*, 1273–1295, doi:10.5194/gmd-5-1273-2012.

Pusz, A. E., R. C. Thunell, and K. G. Miller (2011), Deep water temperature, carbonate ion, and ice volume changes across the Eocene-Oligocene climate transition, *Paleoceanography*, 26, PA2205, doi:10.1029/2010PA001950.

Rose, K. C., F. Ferraccioli, S. S. R. Jamieson, R. E. Bell, H. Corr, T. Creyts, D. Braaten, T. Jordan, P. Fretwell, and D. Damaske (2013), Early East Antarctic Ice Sheet growth recorded in the landscape of the Gamburtsev Subglacial Mountains, *Earth Planet. Sci. Lett.*, 375, 1–12, doi:10.1016/j.epsl.2013.03.053.

Shackleton, N., and J. P. Kennett (1975), Late Cenozoic oxygen and carbon isotopic changes at DSDP Site 284: Implications for glacial history of the Northern Hemisphere and Antarctic, *Init. Rep. Deep Sea Drill. Proj*, 29, 743–755.

Stocchi, P., et al. (2013), Relative sea-level rise around East Antarctica during Oligocene glaciation, *Nat. Geosci.*, 6, 380–384, doi:10.1038/NGEO1783.

Thompson, S. L., and D. Pollard (1997), Greenland and Antarctic mass balances for present and doubled CO_2 from the GENESIS version-2 global climate model, *J. Climate*, 10, 871–900, doi:10.1175/1520-0442(1997)010<0871:GAAMBF>2.0.CO;2.

Wilson, D. S., and B. P. Luyendyk (2009), West Antarctic paleotopography estimated at the Eocene-Oligocene climate transition, *Geophys. Res. Lett.*, 36, L16302, 1–4, doi:10.1029/2009GL039297.

Wilson, D. S., S. S. R. Jamieson, P. J. Barrett, G. Leitchenkov, K. Gohl, and R. D. Larter (2012), Antarctic topography at the Eocene-Oligocene boundary, *Palaeogeogr. Palaeoclimatol. Palaeoecol.*, 335-336, 24–34, doi:10.1016/j.palaeo.2011.05.028.

Zachos, J. C., T. M. Quinn, and K. A. Salamy (1996), High-resolution deep-sea foraminiferal stable isotope records of the Eocene-Oligocene climate transition, *Paleoceanography*, 11, 256–266, doi:10.1029/96PA00571.

Zachos, J. C., M. Pagani, L. Sloan, E. Thomas, and K. Billups (2001), Trends, rhythms, and aberrations in global climate 65 Ma to present, *Science*, 292, 686–693, doi:10.1126/science.1059412.